arXiv:1412.2815v2 [cond-mat.mtrl-sci] 11 Feb 2015

Numerical modeling of the heterocycle intercalated proton-conducting polymers at various mole ratios

T. Masłowski[a,*], A. Drzewiński[a], P. Ławniczak[b], J. Ulner[c]

[a] *Institute of Physics, University of Zielona Góra, ul. Prof. Z. Szafrana 4a, 65-516 Zielona Góra, Poland*
[b] *Institute of Molecular Physics, Polish Academy of Sciences, ul. M. Smoluchowskiego 17, 60-179 Poznań, Poland*
[c] *Institute of Low Temperature and Structure Research PAN, ul. Okólna 2, 50-422 Wrocław, Poland*

Abstract

The kinetic Monte Carlo simulations are employed to study the proton conductivity for anhydrous heterocyclic based polymers. The proton transport is based on a two-step process called the Grotthuss mechanism. In the referring system the proton concentration depends on the relative molar ratio, x, of the benzimidazole and the polystyrene sulfonic acid. Available experimental data with contrasting behavior are fitted and interpreted in terms of our microscopic model. Moreover, it has been shown that the current behavior similar to the Vogel-Tamman-Fulcher law can be reproduced with high precision on the basis of the Grotthuss mechanism.

Keywords: Anhydrous proton conductor, Heterocyclic-based polymers, Kinetic Monte Carlo

1. Introduction

The microscopic modeling of proton transport is one of the long-standing problems in many areas of science ranging from conversion of chemical energy into electrical one to various biological systems [1, 2]. Ice and water became the first hydrogen-bonding systems for which the microscopic description of proton defect transport has been provided in great detail [3]. However, as there are several advantages of fuel cells operating above the boiling temperature of water [4], recently the polymer systems which conduct protons in the absence of any water have become the subject of intensive research. Unfortunately, the proton conductivity of conventional polymer membranes under anhydrous condition is usually very low. Therefore, the promising strategy for the synthesis of new materials was the doping of a high boiling proton solvent into a polymer

*Corresponding author
Email address: T.Maslowski@if.uz.zgora.pl (T. Masłowski)

matrix. Then the proton transport occurs almost entirely through the Grotthuss mechanism, a two-stage mechanism [5, 6], consisting of thermally induced reorientation and proton tunneling in hydrogen bonds (H-bonds).

As is well known, both chemical and physical properties of a polymer material may change with substitution. So to get polymer electrolytes the polymer matrix (e.g., polystyrene, polyacrylate, polysiloxane) is doped by amphoteric nitrogen-based heterocycles (e.g., imidazole, triazole, benzimidazole) at various mole ratios [7–9]. As a result the heterocycles may be covalently tethered to a suitable polymer and linked by the N–H$\cdots$N hydrogen bridges providing a migration path for excess of protons emerging from the dissociation of the acid functions.

For many heterocyclic based polymer proton conductors the temperature dependence of dc conductivity follows at low doping ratios $x \leq 1.0$ (x is the number of moles of heterocycle per polymer repeat unit containing the acidic group) the simple Arrhenius law

$$\sigma = \sigma_0 \exp\left(E_a/k_B T\right), \tag{1}$$

where E_a is the activation energy for proton migration, k_B is Boltzmann's constant and σ_0 corresponds to carrier proton number. But what is intriguing, at a high doping the temperature-dependent conductivity seems to follow the Vogel-Tamman-Fulcher (VTF) law [10–12]

$$\sigma = \sigma_0 \exp\left(E_a/k_B(T - T_0)\right). \tag{2}$$

typically associated with a viscous material whose conductivity is driven by the segmental motions above the glass transition temperature. The parameter T_0 corresponds to the temperature where the free volume disappears. Moreover, for these compounds the crossover driven by the molar ratio is accompanied by an abrupt increase in proton conductivity for $1 < x < 1.5$.

To address this controversy, we have evaluated the experimental data in the wide range of doping ratio [10] employing the model [13] based on the kinetic Monte Carlo (KMC) simulations [14–17] which we describe briefly here. The proton conduction process of the immobilized heterocycles can be considered as a cooperative one involving both molecular motions prior to the proton exchange (by the 180° flip) and migration along the H-bond chain. It can be well modeled by the one-dimensional system of rods each of which has only two positions where the rod ends can be occupied by protons. The key point is to know *a priori* all transition rates from every configuration to any other allowed one [16]. When it is satisfied the KMC method gives the answer to the question of how long the system remains in the same configuration and to what configuration it will evolve [14]. Herein, the rotations, as a sub-process, are treated as a thermally activated process satisfying the Arrhenius law [Eq. (1)] with the activation energy, E_a, given by

$$E_a = \max\left(0, V_{\text{act}} + |e|Kb\right), \tag{3}$$

where V_{act} is the activation energy for rotation in the vanishing electric field, e—the value of the elementary charge, K—the external electric field strength,

and b—the size of the rod. The prefactor σ_0 (in this case called the frequency of rotation ν_R^0) is calculated by solving the Schrödinger equation for the one-dimensional quantum rotor (see [13]).

The migration of a proton from one rod to another represents the hopping between the minima of the H-bond potential. Hopping is defined as the thermally assisted tunneling which is an extension of the purely classical Arrhenius behavior. We approximate the H-bond potential by the fuzzy Morse potentials originating in rod ends as they represent anionic groups between which the H-bonds are created.

$$\begin{aligned} V_a(z) &= \frac{1}{2a}\int_{-a}^{a}\left[V_{\mathrm{Morse}}\left(\frac{d}{2}-z+y\right)\right. \\ &\quad \left. + V_{\mathrm{Morse}}\left(z-y-\frac{d}{2}\right)\right]dy\,, \qquad (4) \\ V_{\mathrm{Morse}}(z) &= g\left[\exp\left(-\frac{2z}{w}\right)-2\exp\left(-\frac{z}{w}\right)\right]\,. \qquad (5) \end{aligned}$$

$V_a(z)$ is the double well potential and the parameter a controls the dispersion in the position of the anionic groups forming the H-bond. Thus, it represents the thermal lattice vibrations. The Morse potential parameters g and w are adjusted to get the distance between the minima of the double well potential V_a equal to Δz together with the height of the barrier equal to h. $V_a(z)$ is used to get quantum analog of the Arrhenius law [18]. In this case the prefactor σ_0, called the frequency of tunneling, is denoted by ν_T^0. More details about the model can be found in our previous paper [13].

This paper is organized as follows: in Sec. 2 the proton concentration with respect to the molar ratio is determined. In Sec. 3 the referring experimental system is presented as well as the simulation results are discussed. Section 4 concludes our paper summarizing the main outcomes.

2. Molar ratio influence on the proton concentration

The blends of polymer and heterocycles are prepared for various x where the result are transparent and homogeneous thin films. The larger ratio x the lower the average distance between the heterocycles, which in turn significantly modifies the character of the H-bond potential. As the amphoteric nitrogen-based heterocycles demonstrate the presence of both protonated and non-protonated nitrogen atoms they can act as donors and acceptors in proton-transfer reactions. Therefore, the change of x affects the concentration of protons, c, on the heterocycle path: a parameter crucial for the proton conductivity ([13], see the inset in Fig. 1).

In order to determine the function $c(x)$ we have performed the numerical simulations considering two types of particles, A and B with the relative ratio x, randomly distributed at sites on a simple cubic lattice. When the adjacent sites are occupied by A and B, they may form a pair (one particle can be paired

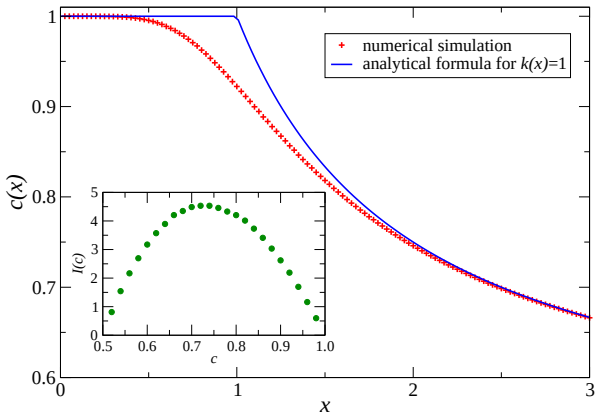

Figure 1: The proton concentration as the function of the molar ratio, the result for the $125\times125\times125$ system. The solid line represents the asymptotic behavior. Inset: The current dependence on the proton concentration [13].

only once). The concentration $c(x)$ may be expressed in terms of the function $k(x)$ describing the probability that A is attached to B:

$$c(x) = \frac{1}{2}\left[1 + k(x)\right] \ . \tag{6}$$

The function $k(x)$ is calculated as the ratio of paired A particles to the number of all A particles. Simulations were performed for system sizes $75 \times 75 \times 75$, $100 \times 100 \times 100$ and $125 \times 125 \times 125$. The function $c(x)$ converges quickly with the system size, providing that the differences between the results for the two largest systems are indistinguishable.

If a simplifying assumption is considered that A is always attached to B, provided that there is a free B particle then simple analytical expressions for asymptotes can be derived: $c(x) = 1$ when x goes to zero and $c(x) = (x+1)/(2x)$ when x is large (see Fig. 1).

In our case A represents a heterocycle while B a polymer unit, and pairing should be understood as forming the anionic group by deprotonation of the acidic group by doping with the heterocycle, e.g., $\mathrm{BnIm} + \mathrm{SO_3H} \rightarrow \mathrm{BnImH^+} + \mathrm{SO_3^-}$ (the benzimidazole is abbreviated to BnIm). In this way some heterocycles are protonated at "free" nitrogen site and the proton concentration increases. The fall of the curve for the increasing x is associated with the relative excess of heterocycles which can hardly come across any free acidic group.

3. Benzimidazole intercalated polymer

In this section the available experimental data for the benzimidazole-based polymer proton conductors [10] are analyzed. For the pure polystyrene the glass-transition temperature is $T_g = 95°\mathrm{C}$ while for the polystyrene sulfonic

acid (PSSA) is shifted to $T_g = 140°C$ [19]. After intercalation of the PSSA within the BnIm, the T_g rises only slightly to 149°C, hardly depending on the molar ratio x. When for the same polymer matrix the imidazole or triazole are dopants they act as plasticizers shifting the T_g values to lower temperatures [20]. Moreover, in such a case the T_g depends significantly on the molar ratio.

The BnIm is anchored to the polymer backbone by the covalent bond. The FT-IR spectra show that the SO_3H groups are deprotonated by doping with the benzimidazole and form SO_3^- groups [10]. This in turn shall increase the concentration of protons traveling along the conduction pathways with respect to the pure BnIm (one proton per one BnIm molecule). But since the highest current was measured at $x = 1.5$, it confirms the well-known fact that the intensive diffusion requires both a high charge density and a high defect density. Note that when the relative molar ratio grows, more and more heterocycles remain not associated with the acidic groups. They are functioning as an insertion into the polymer structure. Because they are not protonated at "free" nitrogen site, such a site provides a defect necessary to have the efficient Grotthuss mechanism.

In our simulations, in general, the parameters have been derived from fitting the experimental data for the proton current at $x = 1.5$ (see Appendix). It should be emphasized that the interplay between the thermal expansion and the thermal vibration [13] is crucial to obtain a high accuracy curve fitting. The parameters of the H-bond potential found for $x = 1.5$ were applied for $x = 1.0$ and 0.5. But when x increases the average distance between benzimidazoles becomes smaller and the activation energy for thermal hopping decreases as well. Similarly, one can expect that the activation energy for rotation of such an unbound heterocycle is lower than that of the immobilized one. So, the effective activation barrier for rotation is likewise to decrease with increasing x. It is also reasonable to expect that when the temperature rises the overall rotational barrier is reduced. Unfortunately, the function describing the change of the rotational potential with increasing temperature is unknown. Therefore, we decided to carry out the simulations for the simplest case when the value of the rotational barrier is independent of temperature.

To verify the role of the activation energy for rotation, our simulations were performed in two ways, namely, the activation energy for rotation was fixed and only the H-bond distance was decreasing with increasing x (Fig. 2a) or it was depended on the molar ratio as well as the H-bond distance (Fig. 2b). The agreement with the experiment is considerably better for the second case.

As one can see in Fig. 2b our microscopic model is able to cover both the Arrhenius behavior for $x = 1$ as well as the VTF-like behavior for $x = 1.5$. It should be emphasized that below the glass transition the current behavior similar to the VTF law can be reproduced with high precision on the basis of the Grotthuss mechanism. Moreover, the best VTF fit in accordance with Eq. (2) exhibits $T_0 = -75$ °C in contrast to the experimental value of the glass transition $T_g = 149$ °C determined by the differential scanning calorimetry. T_0 is the temperature at which the segmental transport ceases to exist and it is extremely hard to believe that this takes place so far below the glass transition [21]. Hence, the VTF-like shape of the conductivity curve does not mean that

we have to deal with the proton transport with the assistance of polymer chain segmental motion.

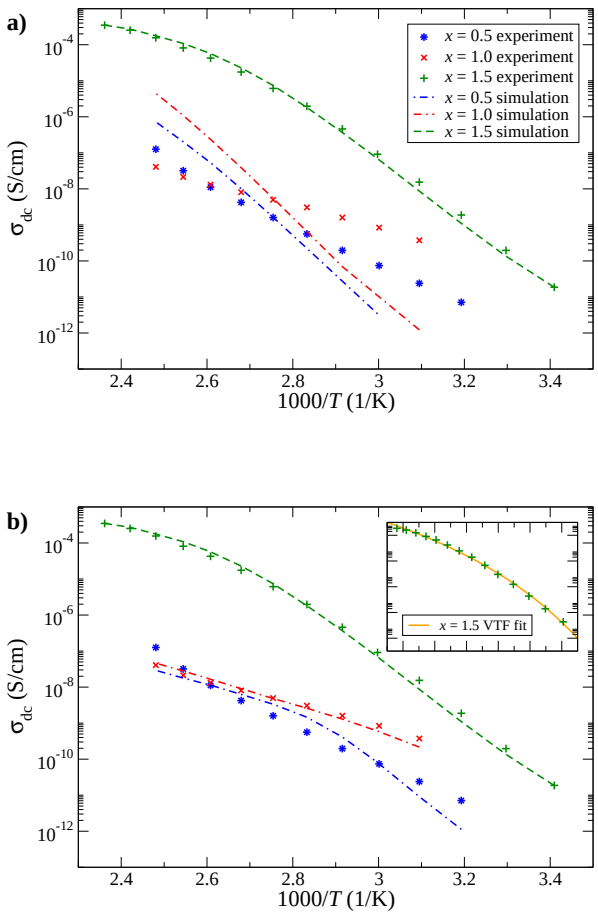

Figure 2: The dashed lines represent the simulation fits, whereas the symbols show the experimental data: a) only the H-bond distance is modified to obtain the best fit, b) both the H-bond distance and the activation energy for rotation are chosen to get the best fit. Specific parameter values are provided in the Appendix. Inset: The best VTF fit to the $x = 1.5$ experimental data. The same scales on the axes as in the main figure.

The numerical results for $x = 0.5$ are moved away from the expected measurement values. This discrepancy is likely to be related to the low concentration of heterocycles making that an unbroken path for the proton transport is formed very rarely. In the percolation terminology it seems to be associated with the

attendance of the percolation threshold for $0.5 < x < 1$. One of the assumptions of our one-dimensional model is the presence of a significant number of conductive paths. Thus, the range of the low molar ratios appear to be beyond the range of applicability of the model.

4. Conclusion

The BnIm intercalated in the PSSA matrix can be employed as the polymer electrolyte membrane holding promise for the synthesis of more temperature tolerant proton conductive membranes. Provided our microscopic approach takes into account the influence of the mole ratio both on the average distance between benzimidazoles, proton concentration and activation energy for rotation we are able to reproduce both measurements following the Arrhenius law and the VTF-like law. Moreover, an abrupt increase in proton conductivity for $1 < x < 1.5$ can be accurately reproduced.

Simulation results for the highest molar ratio ($x = 1.5$) show that the current behavior similar to the VTF law should not always be attributed to segmental motion of the polymer matrix. Sometimes, below the glass transition, a subtle interplay of parameters governing the proton transport can lead to the VTF-like behavior despite the fact that we are dealing only with the Grotthuss mechanism.

As for the polycrystalline benzimidazole the current studies [13] have demonstrated that the thermal lattice vibrations, which modify the H-bond potential, play an essential role in the conduction process. Overall, the validity of the model has been successfully examined for two different systems based on the BnIm. So, it can be concluded that the major diffusion processes have been correctly captured in our model formulation.

Acknowledgments

This work was supported by the Polish Ministry of Science and Higher Education through Grant No. N N202 368139. We have benefited from discussions with Maria Zdanowska-Frączek.

Appendix A. Model parameters

d_0 and a_0 are the values of d and a at $T = T_0$, while d_1 and a_1 are the thermal linear expansion coefficients. The d_0 parameter for $x = 1.5$ case has been chosen to obtain a single representative value of the H-bond length. In order to have a non-vanishing current, the electric field K must be nonzero, but as long as we stay in the linear response regime, which is indeed what takes place in this case, its absolute value has no significant effect on the results. The b and I parameters can be derived from the geometry of the BnIm, ν_R^0 is calculated from V_{act}, whereas other parameters are treated as free (see [13] for details). The best fit parameter values for $x = 1.5$ are presented in Table A.1.

Table A.1: Values of parameters for the PSSA+BnIm simulations.

Parameter	Symbol	Value
Frequency of rotation prefactor	ν_R^0	1.42×10^{12} Hz
Activation energy for rotations	V_{act}	0.45 eV
Rods length	b	3.84 Å
Moment of inertia	I	123.6 u Å^2
External electric field	K	0.005 V/Å
H-bond length	d_0	2.8 Å
Thermal expansion coefficient	d_1	10^{-5} Å/K
V_a barrier height	$h(T_0)$	0.625 eV
Distance between minima of V_a	$\Delta z(T_0)$	0.96 Å
Reference temperature	T_0	293.3 K
D and L defects energy	V_{Coul}	0.4 eV
Frequency of hopping prefactor	ν_T^0	10^7 Hz
Lattice vibration amplitude	a_0	0.8 Å
Thermal susceptibility of a	a_1	0.00093 Å/K

The variable parameters for the various molar ratios:
Fig. 2a:
$x = 1.0$: $d_0 = 2.8375$ Å,
$x = 0.5$: $d_0 = 2.83$ Å.
Fig. 2b:
$x = 1.0$: $d_0 = 2.8075$ Å, $V_{\text{act}} = 0.75$ eV, $\nu_R^0 = 1.82 \times 10^{12}$ Hz,
$x = 0.5$: $d_0 = 2.815$ Å, $V_{\text{act}} = 0.675$ eV, $\nu_R^0 = 1.72 \times 10^{12}$ Hz.

References

[1] P. Colomban, *Proton Conductors: Solids, Membranes and Gels - Materials and Devices* (Cambridge University Press, 1992).

[2] K.-D. Kreuer, Chem. Rev. **104**, 4637 (2004). doi:10.1021/cr020715f.

[3] P. Schuster, G. Zundel and C. Sandorfy, *The Hydrogen Bond. Structure and Spectroscopy* (North-Holland Publishing Company, Amsterdam, 1976), Vol. 2.

[4] I. Honma, M. Yamada, Bull. Chem. Soc. Jpn. **80**, 2110 (2007). doi:10.1246/bcsj.80.2110.

[5] C. J. T. Grotthuss, Ann. Chim. (Paris) **58**, 54 (1806).

[6] K.-D. Kreuer, Chem. Mater. **8**, 610 (1996). doi:10.1021/cm950192a.

[7] K.-D. Kreuer, A. Fuchs, M. Ise, M. Spaeth and J. Maier, Electrochim. Acta **43**, 1281 (1998). doi:10.1016/S0013-4686(97)10031-7.

[8] K.-D. Kreuer, J. Membr. Sci. **185**, 29 (2001). doi:10.1016/S0376-7388(00)00632-3.

[9] S. Ü. Çelik, A. Bozkurt, S. S. Hosseini, Prog. Polym. Sci. **37**, 1265 (2012). doi:10.1016/j.progpolymsci.2011.11.006.

[10] A. Bozkurt, Turk. J. Chem, **29**, 117 (2005).

[11] M. Yamada, I. Honma, Electrochim. Acta **48**, 2411 (2003). doi:10.1016/S0013-4686(03)00263-9; H. Erdemi, A. Bozkurt, W. H. Meyer, Synthetic Met. **B 143**, 133 (2004). doi:10.1016/j.synthmet.2003.10.022; G. Scharfenberger, W. H. Meyer, G. Wegner, M. Schuster, K.-D. Kreuer, and J. Maier, Fuel cell **6**, 237 (2006). doi:10.1002/fuce.200500210; T. Itoh, T. Sakakibara, Y. Takagi, M. Tamura, T. Uno, M. Kubo, Y. Aihara, Electrochim. Acta **55**, 1419 (2010). doi:10.1016/j.electacta.2009.02.030.

[12] J. Vila, C. Franjo, J. M. Pico, L. M. Varela, O. Cabeza, Port. Electrochim. Acta **25** 163 (2007).

[13] T. Masłowski, A. Drzewiński, J. Ulner, J. Wojtkiewicz, M. Zdanowska-Frączek, K. Nordlund and A. Kuronen, Phys. Rev. **E 90**, 012135 (2014). doi:10.1103/PhysRevE.90.012135.

[14] A. B. Bortz, M. H. Kalos and J. L. Lebowitz, J. Comput. Phys. **17**, 10 (1975). doi:10.1016/0021-9991(75)90060-1.

[15] W. M. Young and E. W. Elcock, Proc. Phys. Soc. **89**, 735 (1966). doi:10.1088/0370-1328/89/3/329.

[16] K. A. Fichthorn and W. H. Weinberg, J. Chem. Phys. **95**, 1090 (1991). doi:10.1063/1.461138.

[17] J. Hermet, F. Bottin, G. Dezanneau, G. Geneste, Solid State Ion. **252**, 48 (2013). doi:10.1016/j.ssi.2013.06.001.

[18] R. P. Bell, Proc. R. Soc. London **A 139**, 466 (1933).

[19] C. R. Martins, G. Ruggeri, M-A. De Paoli, J. Braz. Chem. Soc. **14**, 797 (2003); C. R. Martins, F. Hallwass, Y. M. B. De Almeida, M.-A. De Paoli, Ann. Magn. Reson. **6**, 46 (2007).

[20] F. Gögtepe, A. Bozkurt, Ş. T. Günday, Polym. Int. **57**, 133 (2008). doi:10.1002/pi.2335.

[21] R. C. Woudenberg, O. Yavuzcetin, M. T. Tuominen, E. B. Coughlin, Solid State Ion. **178**, 1135 (2007). doi:10.1016/j.ssi.2007.05.006.